

LASER APPLICATIONS AND OTHER TOPICS IN QUANTUM ELECTRONICS

PACS numbers: 42.15.Dp; 42.87.Bg
DOI: 10.1070/QE2005v035n03ABEH002735

Visualisation of the wave-front deformations caused by a phase object by the method of successive double lateral shear interferometry

A.M. Lyalikov

***Abstract*. The method of moire visualisation of the wave-front deformations of a light beam propagated through a phase object is proposed. The method is based on the recording of double shear interferograms and makes it possible to obtain real-time moire pictures of the phase object with doubled sensitivity, in which the behaviour of fringes is similar to that in usual double-beam, reference-wave interferometry. The method was tested by studying the regions of thermal treatment of a polymethyl methacrylate plate.**

Keywords: *phase object, wave front, interferogram, moire picture.*

In some practical cases the shear interferometry is not only inferior to the reference-wave interferometry but even more preferable than the latter. Shear interferometers have a low sensitivity to vibrations and are simple to align. Among the numerous methods for producing the shift between identical wave fronts, the most popular are the methods using lateral shear interferometers [1, 2], which are widely applied at present in different fields of science and technology [3 – 7]. However, a disadvantage of shear interferometry is a complicated interpretation of the interference pattern. The behaviour of the interference fringes obtained by the method of lateral shear interferometry depends both on the relation between the shear and size of the object and the shear itself. If the object occupies only a part of the working field and its size is smaller than the shear, the same interference fringes are obtained as in the double-beam, reference-wave interferometry [8]. This particular case of interferometry deserves a special attention because it combines all the advantages of the two above-mentioned methods. First of all the complexity of interpretation of the interference pattern inherent in shear interferometry is eliminated, and the behaviour of interference fringes directly visualise a change in the wave phase caused by the object.

The use of holographic principles for obtaining lateral shear interferograms and their optical processing considerably expanded the possibilities of shear interferometry [9 – 14], providing the compensation of aberrations of an optical system and an arbitrary adjustment of fringes in the reconstructed interference patterns, as well as an increase in the measurement sensitivity.

In this paper, the method for visualisation of wave-front deformations caused by a phase object is considered. The method is based on the recording of double-shear interferograms and is applicable when the lateral shear exceeds the size of the phase object. In this case, the transverse size of the object itself in the shear direction should not exceed 1/3 of the diameter of a probe light beam. The method allows one to obtain real-time moire pictures of the phase object with doubled sensitivity, in which interference fringes are similar to those obtained in usual double-beam, reference-wave interferometry.

Figure 1 shows the scheme explaining the moire method for visualisation of the wave-front distortions caused by the phase object with the help of successive double lateral shear interferometry.

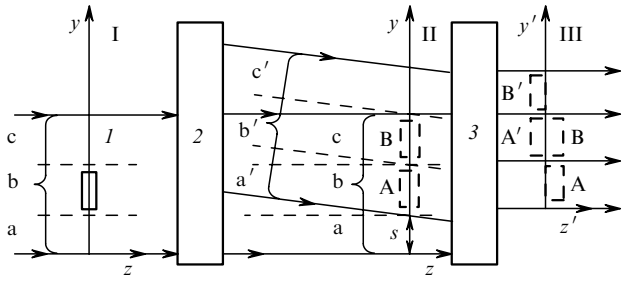

Figure 1. Scheme of the method: (*1*) phase object under study; (*2*, *3*) lateral shear interferometers.

Let us assume that phase object under study (*1*) (Fig. 1) is located in the central region of a probe light beam and its transverse size in the direction of the shear between interfering beams does not exceed 1/3 of the light-beam diameter. In this case, the shear s can be equal to 1/3 of the light-beam diameter.

The coordinate system x, y in output plane I (Fig. 1), where phase object (*1*) is located, is selected so that the y axis coincides with the direction of the shear between interfering beams, which is specified by shear interferometer (*2*). The z axis coincides with the probe-beam direction. To describe the phase distortions of wave probing phase object (*1*), it is convenient to divide the wave surface into three regions of width s along the y axis. The boundaries of these regions a, b, and c are indicated by the dashed straight lines in Fig. 1. In regions a and c, the wave surface is unper-

A.M. Lyalikov Yanka Kupala Grodno State University, ul. Ozheshko 22, 230023 Grodno, Belarus; e-mail: lyalikov@inbox.ru

Received 28 May 2004
Kvantovaya Elektronika **35** (3) 290 – 292 (2005)
Translated by M.N. Sapozhnikov

turbed. If the probe beam propagates strictly along the z axis and has a plane wave front, the distortions of its phase $\Phi(x, y)$ caused by the phase object can be written in the form

$$\Phi(x, y) = \begin{cases} \text{const for regions a, c,} \\ \varphi(x, y) \text{ for regions b,} \end{cases} \quad (1)$$

where $\varphi(x, y)$ are the phase distortions characterising the deformation of a plane wave front of the probe beam caused by phase object (*1*).

An important feature of this method is that the lateral shear interferogram being formed in plane II (Fig. 1) should be adjusted to the interference fringes of a finite width. The lateral shear interferogram is formed due to the superposition of two waves propagated through the phase object. Phase distortions $\Phi_1(x, y)$ for the first wave are described by expression (1) with an accuracy to a constant phase and for the second wave (due to the tilt of the light beam upon adjustment to the fringes of a finite width) by the expression

$$\Phi_2(x, y) = \begin{cases} 2\pi\eta y \text{ for regions a}', \text{ c}', \\ 2\pi\eta y + \varphi(x, y - s) \text{ for the region b}', \end{cases} \quad (2)$$

where a′, b′, and c′ are the corresponding surface regions in the shifted beam; $\eta = (\cos\beta)/\lambda$; β is the angle between the beam direction and y axis; and λ is the wavelength. To simplify the description of the method, we assume that the interfering beams are located in the yz plane.

One can see from Fig. 1 that the lateral shear interference pattern in plane II is formed in the region A due to the superposition of the perturbed region b of the first wave with phase distortions $\Phi_1(x, y)$ and the unperturbed region a′ of the second wave with phase distortions $\Phi_2(x, y)$, while in the region B this pattern is formed due to the superposition of the unperturbed region of the first wave and the perturbed region b′ of the second wave. To exclude effects related to the refraction of light beams in phase object (*1*), plane II of the lateral shear interferogram and object plane I are made optically conjugated.

As a result, the behaviour of interference fringes in the regions A and B will visualise the function $\varphi(x, y)$ determining the deformation of a pane wave front by the phase object. This is confirmed by the lateral shift interferogram (Fig. 2) obtained upon adjusting to an infinitely broad fringe [$\eta = 0$ in (2)]. As a phase object, a thermally processed polymethyl methacrylate plate was used. The size of the thermally processed region (the width of the region A or B) did not exceed the lateral shear between interfering beams. One can see from the interference pattern that the fringes in regions A and B are virtually identical (accurate to uncompensated aberrations).

The method of double successive shear in plane II realises the shear interferogram adjusted to finite-width fringes. Taking into account (1) and (2), the intensity distribution in such an interference pattern can be written in the form

$$I(x, y) \sim \begin{cases} \cos^2\left[\pi\eta y - \frac{1}{2}\varphi(x, y)\right] \text{ for the region A,} \\ \cos^2\left[\pi\eta y + \frac{1}{2}\varphi(x, y - s)\right] \text{ for the region B,} \end{cases} \quad (3)$$

The interference fringes of this interferogram are oriented perpendicular to the y axis and their period is $1/\eta$.

Figure 2. Lateral shear interferogram of a polymethyl methacrylate plate obtained by adjusting to an infinitely broad fringe.

Then, the two images of the interference pattern of type (3) are superimposed with the help of second lateral shear interferometer (*3*) (Fig. 1) in plane III optically conjugated with plane II. The images are shifted with respect to each other along the y' axis by the value s so that the region A′ of the pattern obtained in the second interferometer overlaps the region B in another interference pattern. To simplify the description of the moire pattern, the z' axis is shifted with respect to the z axis by the value s, as shown in Fig. 1.

The superposition of interference patterns adjusted to the finite-width fringes gives the moire pattern in plane III. To simplify the interpretation of moire fringes, it is desirable to violate coherence between pairs of beams forming shifted interference patterns in plane III. This can be achieved by placing a diffusion scatterer (ground glass) in the plane II and by forming a lateral shear interference pattern (3) on it. The, by neglecting the effects of formation and interference of speckle structures [15], we obtain the intensity distribution in the moire pattern in plane III

$$I(x, y) + I(x, y + s) \sim \cos^2\left[\pi\eta y - \frac{1}{2}\varphi(x, y)\right] \times \cos^2\left[\pi\eta y + \frac{1}{2}\varphi(x, y)\right] \sim I_\Sigma(x, y) + \cos(2\pi\eta y)\cos\varphi(x, y), \quad (4)$$

where $I_\Sigma(x, y)$ contains the terms that are insignificant for the description of the moire pattern. The system of moire fringes represents the regions of the image in which the visibility of superimposed interference fringes with the period $1/\eta$ is zero. The visibility of the interference fringes is minimal when the second cosine in expression (4) vanishes. Therefore, the equations of the family of moire fringes observed in plane III can be represented in the form

$$\varphi(x, y) = \pi\left(N + \frac{1}{2}\right), \quad (5)$$

where $N = 0, 1, 2, \ldots$ is the number of a moire fringe. Expression (5) corresponds to the centre of the moire fringe.

One can see from (5) that the moire pattern directly visualises the function $\varphi(x, y)$ describing the wave-front deformation by the phase object. Note here that the distance between the moire fringes corresponds to a change in the phase distortion $\varphi(x, y)$ by π rather than by 2π, as in case of the double-beam, reference-wave interferometry. This demonstrates that the sensitivity of the moire pattern is twice as high as that of the interference pattern obtained by the method of double-beam, reference-wave interferometry.

Figure 3 shows the moire picture of the polymethyl methacrylate plate obtained by the method described above. The four-mirror Mach – Zehnder interferometers were used as shear interferometers (*2*) and (*3*) (Fig. 1), which can control both the lateral shear and period of interference fringes. The fringe period in the shear interferograms recorded in plane II was 0.25 mm. A comparison of the moire pattern (Fig. 3) and the lateral shear interferogram (Fig. 2) shows that the number of fringes in the former also doubled due to its doubled sensitivity.

Figure 3. Real-time moire pattern visualising with doubled sensitivity the distortions of the probe-wave phase propagated through a polymethyl methacrylate plate.

References

1. Waetzmann E. *Annalen der Physik*, **39**, 1042 (1912).
2. Malakara D. (ed.) *Opticheskii proizvodstvennyi kontrol'* (Optical Industrial Control) (Moscow: Mashinostroenie, 1985).
3. Shekhtman V.N., Rodinov A.Yu., Pel'menev A.G. *Opt. Spektrosk.*, **76**, 988 (1994).
4. Bashkin A.S., Korotkov P.I., Maksimov Yu.P., et al. *Kvantovaya Elektron.*, **24**, 786 (1997) [*Quantum Electron.*, **27**, 766 (1997)].
5. Santhanakrishnan T., Palanisamy P.K., Sirohi R.S. *Appl. Opt.*, **37**, 3447 (1998).
6. Schwider J. *Optik*, **108**, 181 (1998).
7. Sokolov V.I. *Kvantovaya Elektron.*, **31**, 891 (2001) [*Quantum Electron.*, **31**, 891 (2001)].
8. Komissaruk V.A., in *Issledovaniya prostranstvennykh gazodinmicheskikh techenii na osnove opticheskikh metodov. Trudy VVIA im. N.E. Zhukovskgo* (Studies of Spatial Gas-dynamic Flows by Optical Methods. Proceedings of the N.E. Zhukovsky All-Union Higher Engineering Academy) (Moscow, 1971) p. 121.
9. Kulkarni V.G. *Opt. and Laser Technol.*, **11**, 269 (1979).
10. Vest C.M. *Holographic Interferometry* (New York: Wiley, 1979; Moscow: Mir, 1982).
11. Gusev V.G. *Opt. Zh.*, **64**, 48 (1997).
12. Toker G., Levin D. *Appl. Opt.*, **37**, 5162 (1997).
13. Lyalikov A.M. *Opt. Spektrosk.*, **93**, 517 (2002).
14. Lyalikov A.M. *Opt. Spektrosk.*, **96**, 148 (2004).
15. Francon M. *Laser Speckle and Applications in Optics, transl. from the French* (New York: Academic Press, 1979; Moscow: Mir, 1980).